

DesignCon 2009

Crosstalk In Via Pin-Fields, Including the Impact of Power Distribution Structures

Gustavo Blando, Sun Microsystems, Inc
Tel: (781) 442 3481, e-mail: gustavo.blando@sun.com

Jason R. Miller, Sun Microsystems, Inc

Douglas Winterberg, Sun Microsystems, Inc

Istvan Novak, Sun Microsystems, Inc

Abstract

Carefully managed escape via allocation in pin field arrays are often necessary in order to avoid excessive crosstalk in high speed interconnects. Vias inject energy into cavities; these cavities in turn transfer energy to its surrounding medium, such as power-plane openings, power, ground, and ultimately other signal vias producing unwanted crosstalk. In this work, we'll study how this coupling mechanism occurs assuming imperfect plane pair cavities and we'll show how ground, and more importantly the plane connections of power vias, might affect, and in some cases amplify crosstalk levels.

Author(s) Biography

Gustavo Blando is a Staff Engineer at Sun Microsystems, with over 10 years of experience in the industry. Currently at Sun Microsystems he is responsible for the development of new processes and methodologies in the areas of broadband measurement, high speed modeling and system simulations. He received his M.S. from Northeastern University.

Jason R. Miller is a senior staff engineer at Sun Microsystems where he works on ASIC development, ASIC packaging, interconnect modeling and characterization, and system simulation. He has published over 30 technical articles on the topics such as high-speed modeling and simulation and co-authored the book "Frequency-Domain Characterization of Power Distribution Networks" published by Artech House in 2007. He received his Ph.D. in electrical engineering from Columbia University.

Douglas Winterberg is a Signal Integrity Engineer at Sun Microsystems with over 10 years experience in systems and interconnect design. Currently he works on system modeling, simulations and validation of high speed interconnects on Sun's time to market server platforms. He received his BS from the Rochester Institute of Technology.

Istvan Novak is a distinguished engineer at Sun Microsystems, Inc. Besides signal integrity design of high-speed serial and parallel buses, he is engaged in the design and characterization of power-distribution networks and packages for Sun servers. He creates simulation models, and develops measurement techniques for power distribution. Istvan has twenty plus years of experience with high-speed digital, RF and analog circuits, and system design. He is a Fellow of IEEE for his contributions to the fields of signal-integrity, RF measurements, and simulation methodologies.

1.0 Introduction

Vias are one of the most interesting and variable-rich passive elements in board interconnects, in many cases contributing to the highest percentage of the channel-loss-budget. Recent publications have shown that cavities play an important role in the via model [1], [2].

Once the cavities are excited, they transfer energy to it's surrounding medium, such as plane openings, other power, grounds, signal vias and plane boundaries, etc. This precise phenomenon is what makes via models so complex and multidimensional. For example, have you ever wondered:

- What is the difference between a signal via in isolation vs. a signal via within a pin-field array?
- How other grounds, and more importantly other power vias, might affect the insertion loss and crosstalk behavior between signal vias?
- How does the plane perforation of a pin-field array diverge from the ideal full plane approximation when modeling vias?

In this work, we'll concentrate on via crosstalk within pin-fields. We'll look at different pin field configurations and show how crosstalk can easily propagate if the pin arrangement has not been properly chosen; how power vias, and the attachment of these power vias to different layers within the stack plays a key role for crosstalk between signal vias. We'll show how all these effects are heavily frequency dependent, having complete isolation at some frequencies, and full coupling at others.

The paper is divided into four sections. Section one is this introduction. In section two we'll review the cavity equation and a simple via theoretical model to understand the fundamentals of how energy is transferred between vias. We'll also explain the importance of the boundary condition in these types of problems, showing how sometimes the boundary effect is so big that it masks the small differences between crosstalk cases. We'll introduce, through simulations, how the cavity resonances are modified when the planes are heavily perforated, as is the case of a signal via in the middle of via field array.

In section three we'll show several test board measurements for a differential pair with various ground configuration patterns. We'll use these measurements to understand how crosstalk between vias is impacted by the proximity of ground vias. We'll also show the same type of measurements, but in heavily perforated areas. Measurement correlations of a few cases will be performed using a 3D field simulator.

Finally in section four, we will extend simulations to include realistic cases involving two differential pairs. We'll show how crosstalk appreciably changes for different ground and power via configuration patterns. More importantly it'll be shown how power vias can resonate and help propagate crosstalk depending of the power via connection layer.

2.0 Cavity Theory Review

As the demand for more integration and higher speed continues to increase, multilayer boards must grow in the number of signal layers to allow for proper routing. Similarly, the number of power and ground planes must increase to allow for proper power distribution and high speed return current paths. Every time planes are facing each other, cavities are created. These cavities transfer energy in all directions from the excitation point and play a paramount role in the coupling between vias. In this section, through simple examples, we'll show this coupling mechanism

2.1 Cavity Analytical Equation and 3D Simulations

Plane pair cavities can be viewed as two dimensional transmission lines, when excited they transmit energy in all directions. These cavities can be simulated with field solvers, but they can also generally be modeled using the well known double summation cavity impedance formula as shown in Equation 1. The plane equation calculates the cavity impedance based on location and boundary condition. For more detail, please refer to references [3], [4].

$$Z_{ij}(\omega) = Z(\omega) \sum_{n=0}^{\infty} \sum_{m=0}^{\infty} \frac{\mathcal{X}_{nm}^2}{w_x w_y (k_{xm}^2 + k_{yn}^2 + Z(\omega)Y(\omega))} f(x_i, y_i, x_j, y_j) \quad (1)$$

Throughout this paper, the cavity equation will be used mostly for cross-checking and validation. CST Microwave Studio simulations and lab measurements will be used to analyze most of the problems. In order to establish an initial baseline and correlate the first simple cavity 3D model, a simple deck (Figure 1) was created and compared to the cavity analytical equation.

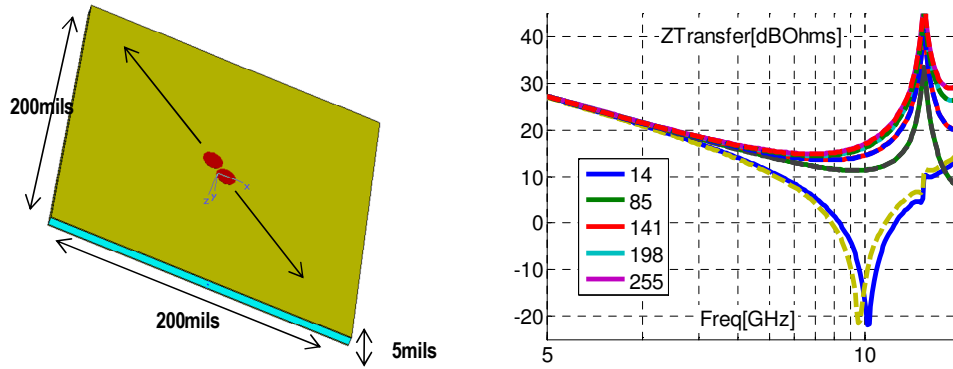


Figure 1: (Left) 200mils x 200mils x 5mils plain pair. Ports diagonally placed from the center. (Right), correlation between the 3D simulations and the analytical expression, (solid - 3D simulations, dashed - double summation Equation 1)

Several simulations were done with various port separations. The ports were moved symmetrically and diagonally from the center. The transfer impedance in [dBOhms] from port-1 to port-2 was computed. An integration range $m=n=10$ with magnetic boundary was used, meaning that at DC we expect to see “infinite” impedance as shown on the trend of the above curve. The first minimum represents a series resonance. When both ports are closely spaced, we see a minimum with a high Q. As we move the ports further away from each other, we can see the Q-factor decreasing due to the positional frequency dependence of the series resonance minimum. The positive impedance peaks, at approximately 15GHz are the first parallel cavity resonance related to the half-wave cavity propagation delay and hence directly proportional to the plane size. The first parallel resonance depends on the plane size, but not the port location, so these peaks are always at the same frequency regardless of the port spacing.

On the curve shown, the 3D field simulations (solid traces) have been plotted on top of the analytical equation results (dashed traces). The correlation is very good although we see a small variation for the 14mil port separation series resonance. This can be traced back to mesh density.

The excellent correlation between the 3D simulation results and the analytical equation builds trust in the selected 3D simulator settings and decks to construct more complex problems with a higher confidence level.

2.2 Via-Cavity Model review

Vias provide the means of sending energy between different layers. Naturally, the injected current transverses cavities; these cavities are exited and the energy contained within is sent into the surrounding medium. Figure 2 depicts this mechanism.

Let’s say we have two vias crossing through a simple two layer stack. When a current is injected on one via, that current will develop a voltage on the plane cavity at the via location. In turn, this “induced” voltage will generate a current that will depend on the plane self impedance at that particular location.

At this point we have injected energy that will propagate on the cavity in all directions encountering different types of obstacles, other vias for example. Every time another via is encountered and a current path is found, the voltage developed

at that location, which is dependent on the transfer impedance between the source and destination location, will generate a current sending energy to somewhere else in the circuit.

In many cases this coupling is intentional as is the case of a differential pair between the “P” and “N” legs. In other cases this coupling is unintentional, and unfortunately many times unavoidable, as in a very dense BGA via field. Ultimately, the plane cavity is the predominant means by which the energy is coupled between vias.

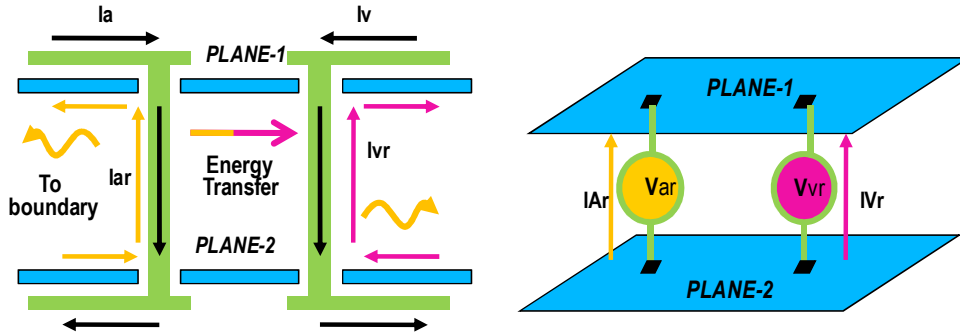


Figure 2: (Left) Physical representation of the coupling between vias. (Right) Circuit representation of the coupling between vias.

When performing simulations, modeling, or even thinking about these type of problems, it’s important to realize that the energy on the cavity propagates in all directions and often times most of the energy reaches the boundary of the structure. Incorrect boundary consideration might produce results very different from reality. A mathematical model using this coupling mechanism has been previously presented in [1],[2]. This model with slight modifications will be used later in this study.

2.3 Field Plot Visualization

For passive interconnects, S-parameters are the de-facto means of analyzing data. When running 3D field simulations of plane cavities, S-parameters can be exported directly from the tools. The [Z] impedance matrix results of the analytical equation can be easily converted to S-parameters.

On an S-parameter simulation, the method normally consist of selecting a predefined set of port locations to calculate the frequency dependent S-parameters. The results will show S-parameters *only* at the port locations

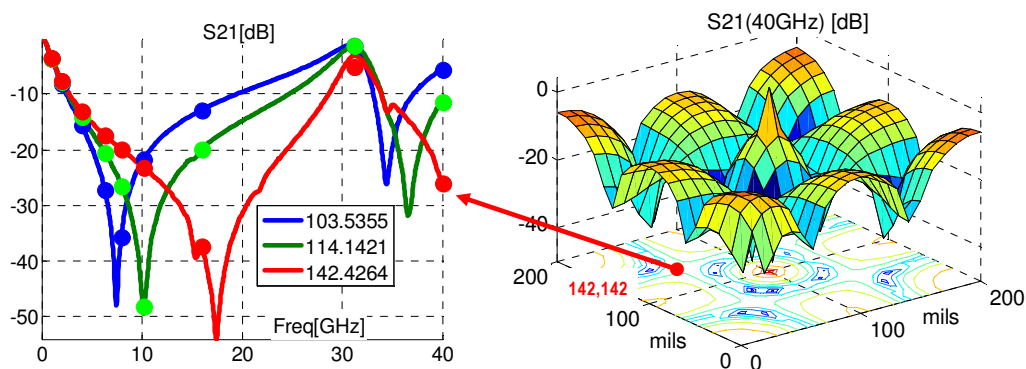


Figure 3: (Left) (solid-trace) S-parameters extracted using discrete ports and (markers) S-parameters calculated at different frequencies on a diagonal plane line from the E-Field. (Right) Calculated S-parameter surface at 40GHz on a 200x200x5mil cavity.

Often times it is useful to view S-parameters at all locations simultaneously. Most of the commercially available field-solvers can plot fields at particular frequencies in the structure volume, but not S-parameters. For cavities however, when the cross-sectional dimension is much smaller than the shortest wavelength of interest, it's rather simple to convert the E-fields to voltages, and ultimately to S-parameters. For thin cavities with the E field mostly perpendicular and constant between the planes at any particular location, Equation 2 can be used to convert from E to S-parameters directly, where "z" represents the chosen port impedance, "th" the cavity thickness, and |Ez| the absolute value of the z component of the Electric field, (perpendicular to the planes).

$$S21 = 20.\log\left(\frac{|Ez|.th}{\sqrt{z}}\right) \quad (2)$$

Even though this is an approximation and its accuracy will depend on the cavity uniformity (proximity to vias will make the E diverge from perpendicular), generally it's very useful and allows us to understand how positional crosstalk varies on any given cavity structure. We'll use this method in follow up sections to show the positional crosstalk in cavities.

2.4 Boundary Effects

As mentioned previously, the boundary effect plays a very important role in all these simulations. To highlight its importance, two simulation decks were created using the 200x200x5mil plane described in Figure 1. In one case, an absorbing boundary (no reflection from the boundary) was used, and in the other a magnetic wall boundary was used (similar to leaving the planes open except fringing effects).

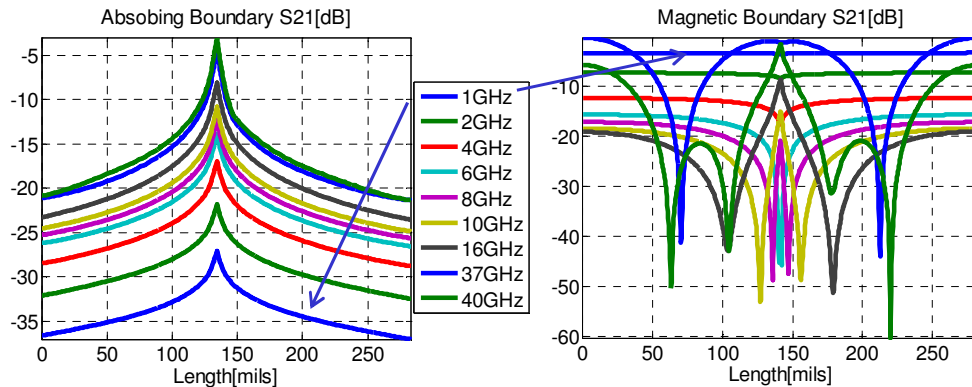


Figure 4: (Left) Cavity coupling at different frequencies using absorbing boundary. (Right) Cavity coupling at different frequencies using magnetic boundary

By using Formula 2 the S-parameters were directly calculated from the E-field and plotted on the diagonal dimension of the plane. This method allows us to have a positional view of how the crosstalk (S21 in this case) behaves as a function of diagonal distance on the plane.

For a magnetic, highly reflective boundary we see that at low-frequency (1GHz) the same amount of coupling is observed across the plane distance. This is due to the fact that all the energy is reflected at the boundaries and the wavelength is large as compared to the plane dimensions. In contrast the coupling of frequencies greater than 6GHz, where the signal wavelength and plane dimensions are of the same order of magnitude, experience peaks and valleys due to the constructive and destructive summation of the incident and scattered waves present on the planes.

An absorbing boundary is a mathematical construct that does not reflect energy, hence appearing as if the planes continue to infinity (no scattered waves). In this case, we observe that the coupling behavior completely reverses. At lower frequencies we have the least amount of coupling since the cavity propagation mode is ill prepared to propagate low frequency signals. Conversely, higher frequencies are propagated strongly on thin cavities. In this case we can also observe the monotonic decay of the coupling as we move further away from the excitation point.

Now, imagine for a moment you are simulating a via located somewhere in this cavity. It's clear that your results will dramatically change depending on the boundary condition selected. In most cases the boundary will be the dominant effect on the results, so careful consideration selecting the boundary is required prior to running simulations.

2.5 Ground Isolation

In order to provide isolation between signal vias within a pin field, ground vias can be placed in between signals. By doing so, the current will tend to return through these ground vias and not propagate to undesired locations on the board

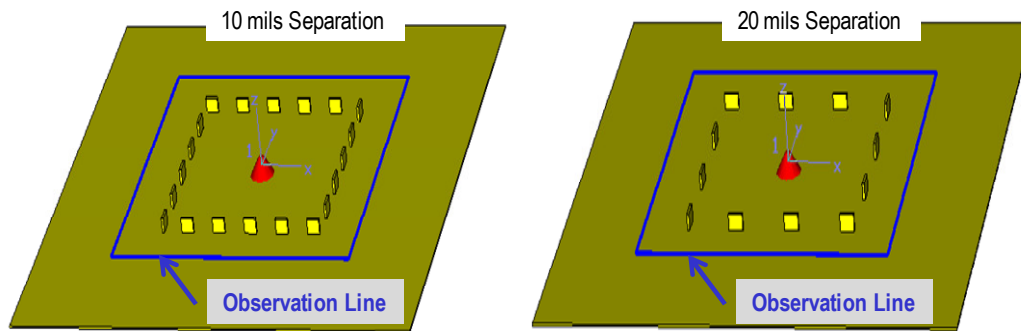


Figure 5: (Left), cavity with a wall of ground blades, separated by a 10mil opening. (Right), cavity with a wall of ground blades, separated by 20mils. In both cases, the plane above was hidden to aide with the physical structure visualization.

In order to conceptually capture this behavior, a simulation was set up using a simple two stack board with small ground blades to short the planes together. As Figure 5 shows, a wall with ground blades was created surrounding an excitation port at the center of the board. Two cases were simulated, one with a blade separation of 10mils, and another with the blades separated 20mils from each other.

Each side of the wall was 80mils long. In both cases an observation line was arranged 20mils outside of the wall in all directions to compute the cavity coupling. The fundamental idea is to observe and estimate how much coupling we might see leaking in between the ground blades at different frequencies. The coupling was computed at 8GHz, 16GHz, 30GHz and 40GHz. These problems were simulated using both an absorbing and magnetic boundary in order to determine how much of an effect the boundary might have when we have ground connections.

Figure 6 shows the results of the absorbing boundary condition for all frequencies and cases (no-wall, 10mil separation and 20mil separation). The amount of coupling for the non-wall case (blue lines) is similar at all frequencies, with the most coupling at 40GHz and the least at 8GHz. This occurs because the observation line is relatively close to the center, hence the difference in attenuation so close to the excitation point is relatively small. If we compare the no wall baseline against the 20mil or the 10mil ground blade separation cases, we can see that the highest isolation happens at 8GHz where the wavelength is big as compared to the small separation between the blades; in essence the wall looks almost solid. It can also be seen that the 40GHz case is the one with the least amount of isolation, since the wavelength at this high frequency is small and more energy can leak between the ground blades. In terms of just absolute value, we can see that 40GHz is also the one leaking the highest amount of energy, as expected.

The four bumps on the curve indicate the observation line is surrounding all four sides of the wall and since the problem is symmetrical we see these four repeated field distributions, one per wall side.

Another very telling exercise is to look at the fields directly. In Figure 7 the fields are plotted for the 20mil ground blade separation case using the same frequencies as Figure 6. The trends explained in Figure 6 can be observed clearly in the fields. Note how the wall, even with 20mil ground blade separation, is successfully containing the 8GHz wave. Conversely, note how at 40GHz the fields leak through the blades leading to additional coupling further away from them.

If the planes are not properly terminated, pin fields close to board edges might experience reflections from an open boundary. Figure 8 depicts the same type of simulations as the absorbing boundary, except now a magnetic boundary is used at the edge of the planes.

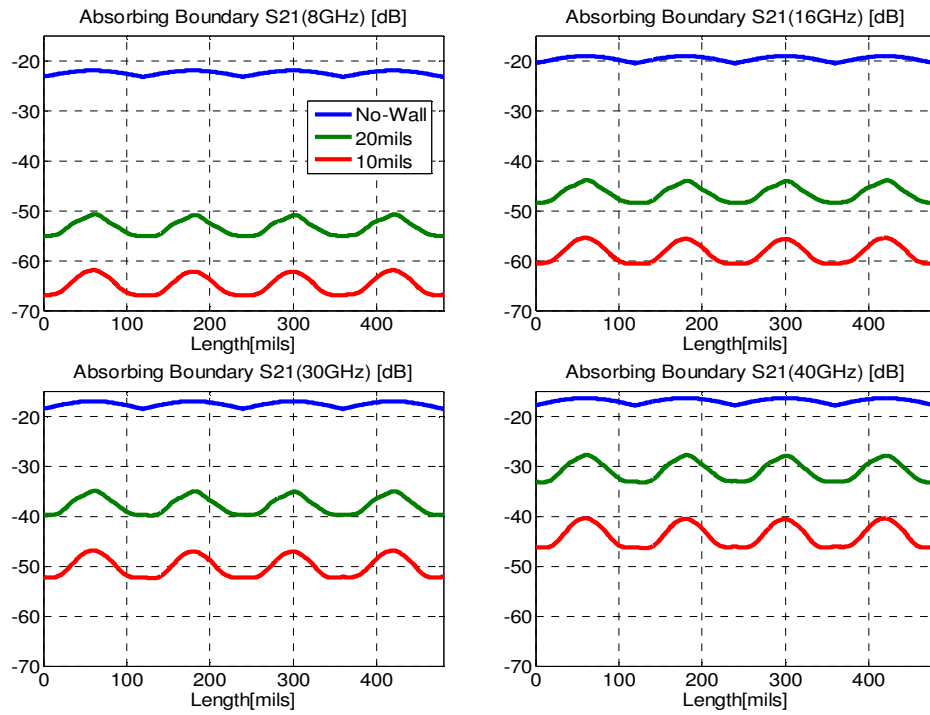


Figure 6: Cavity coupling at (Top-Left) 8GHz, (Top-Right) 16GHz, (Bottom-Left) 30GHz, (Bottom-Right) 40GHz, using an absorbing boundary with an observation line 20mils outside the ground blade wall

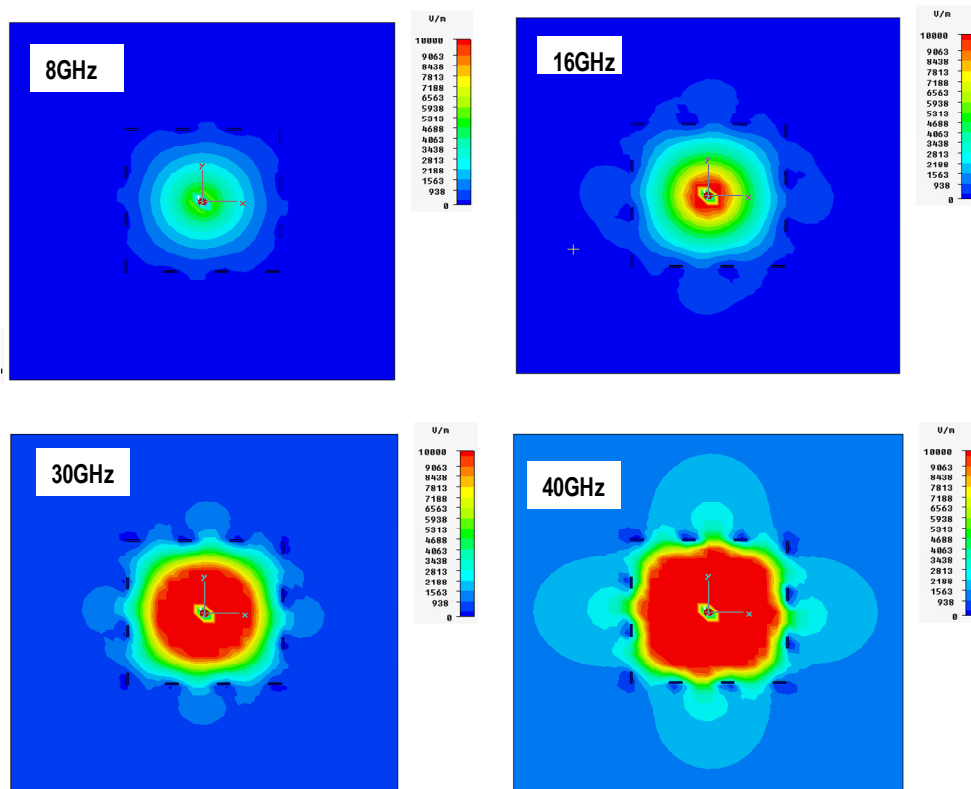


Figure 7: Electric field distribution at (Top-Left) 8GHz, (Top-Right) 16GHz, (Bottom-Left) 30GHz, (Bottom-Right) 40GHz, using an absorbing boundary with 20mil ground blade separation

It can be seen that at 8GHz the isolation is good and all three cases are similar to the absorbing boundary simulation. This is as expected since all the energy at this low frequency is contained within the ground blade wall and very little energy is sent to the boundary to reflect. At 16GHz we start to see how the profile starts to get distorted. This is an indication that some leakage is getting through the blades and into the boundary.

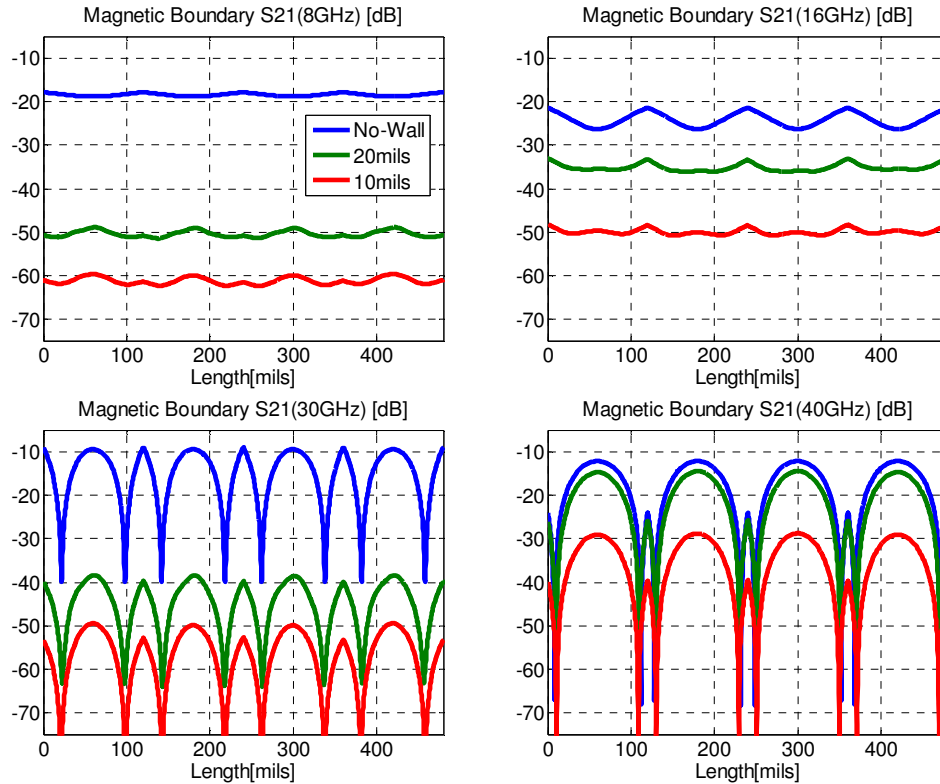


Figure 8: Cavity coupling at (Top-Left) 8GHz, (Top-Right) 16GHz, (Bottom-Left) 30GHz, (Bottom-Right) 40GHz using a magnetic boundary with an observation line 20mils outside the ground blade wall

Finally for the 30GHz and 40GHz cases we see that a lot of energy is reaching the boundary that reflects and distorts the clean profile of the absorbing boundary. Note how at 40GHz the ground blades with 20 mil separation almost do not serve as a shield and the result is on top of the baseline. While this is just a theoretical example, it highlights the importance of the proper boundary condition consideration when analyzing these problems. As shown in Figure 8, the 40GHz case is dominated by the boundary.

The fields for the magnetic boundary were also plotted. A significant difference can be seen between the 8GHz and 40GHz cases. On the 40GHz case the resonance patterns can be observed, while at 8GHz the containment of the fields within the walls is evident. In all the field plots the scale has been kept constant so a relative comparison can be made visually.

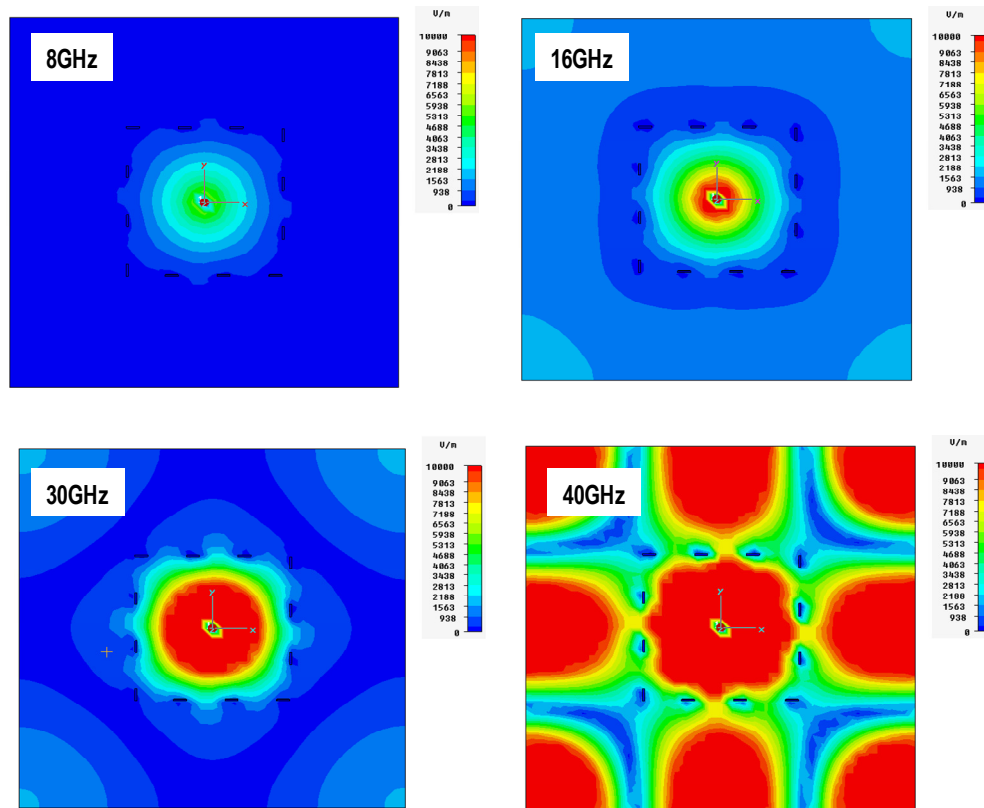


Figure 9: Electric field distribution at (Top-Left) 8GHz, (Top-Right) 16GHz, (Bottom-Left) 30GHz, (Bottom-Right) 40GHz using a magnetic boundary with 20mil ground blade separation

2.6 Another Way to Look at Via Return Currents

Up to now, cavities have been analyzed by placing the ports directly between planes, forcing a voltage and injecting a pre-defined amount of energy into the cavity. Signal vias, rather than connecting directly to the planes, transverse them inside anti-pad openings. The energy injected into its cavity is induced, based on the physical dimensions of the via, instead of forced between planes by direct port connections.

The previously used generic cavity simulation deck was slightly modified, as shown in Figure 10, to mimic a signal via transition with the proper port connections. A solid ground blade wall surrounding the signal via was added and several simulations were performed to highlight the effect of the via return current path. The wall size was swept from 10mils to 80mils of length per side.

The objective of this exercise is to illustrate how the current return path is generated for a signal via transition. The simulation results in Figure 10 show that the signal propagation is very good up to 30GHz when the wall is close to the via. The concept of the ground blade as an ideal return path, as if the via and return wall were a uniform transmission line structure, is valid in this case. As we move the ground blade farther away, oscillations appear in the insertion loss profile, and at the 70mils and 80mils ground blade separations abrupt resonances start to show up.

The point to take away is that in via structures the cavity is the means of energy propagation. A via surrounded with a closed ground wall shorting the planes, acts as an electrical boundary, reflecting all the energy and developing half wave resonances based on the diagonal dimension of the closed boundary.

When the surrounding ground wall is spaced close to the signal via, the cavity resonances are observed only at very high frequencies despite their presence. When the ground wall is spaced farther away from the centered via, the diagonal

dimension of the plane cavity enclosed by the surrounding wall increases, lowering the half wave resonance and making it visible at lower frequencies.

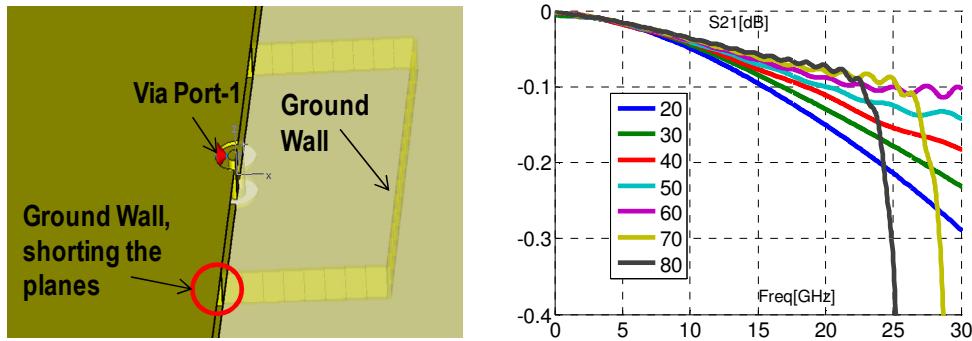


Figure 10: (Left) Physical structure of a via with a close ground wall. (Right) S-parameters results for different ground wall dimensions

At the half wave resonance frequency for a centered via within the ground wall, a maximum impedance will be present between the planes exactly at the signal via location. The cavity's high impedance, located at the signal via's return current path, dramatically increases the insertion loss as can be seen on the 70mils and 80mils cases in Figure 10.

2.7 Perforated Planes

In pin-field locations, planes are sometimes heavily perforated, and in many cases the perforation leaves more voids than copper. Reference [5] demonstrates that as we move further into a pin-field array the plane impedance increases. In this section, we'll apply simple simulations in an attempt to understand how the cavity behavior changes depending on the size and number of perforations. For simplicity, square holes have been used. The trends observed with the simulated square perforations will be similar to the more realistic circular “anti-pad” shapes.

Various 3D field simulation structures were created as follows:

- 5% cut area, with 6,10 and 14 holes per side (a total of 36, 100 and 196 holes respectively). Naturally in order to get the same % area cut, each case will have a different size square hole
- 25% cut area, with 6,10,14 holes per side
- 50% cut area, with 6,10,14 holes per side

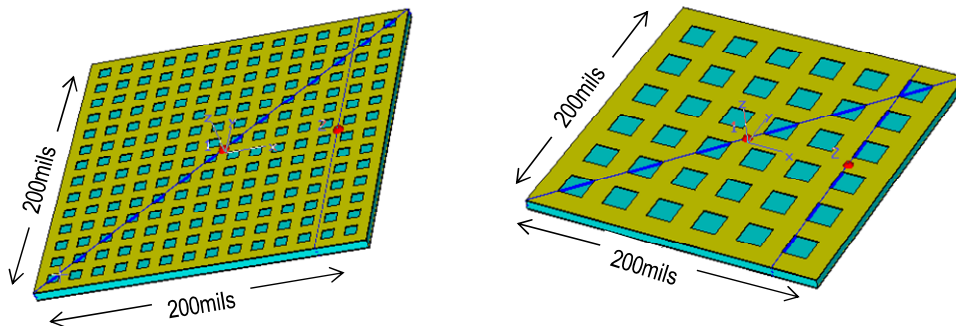


Figure 11: (Left) Perforated plane, with 14 holes per side and 25% copper area removed. (Right) Perforated plane with 6 holes per side and 25% copper area removed

Figure 11 shows the 25% cut case having 14 holes per side (left), and only 6 holes per side (right). In order to keep the same percentage cut between different numbers of perforation, the holes sizes had to change. The excitation port is located at the center of the structure, and the response port is located 71mils away from the center. The plane pair is 200x200x5mil in size and all simulation decks used a magnetic boundary.

For the same perforation percentage, the smaller number of holes (largest size) push the parallel and plane series resonances to a lower overall frequency as shown on Figure 12. This is observed for the 50%, 25% and 5% cases (5% not shown).

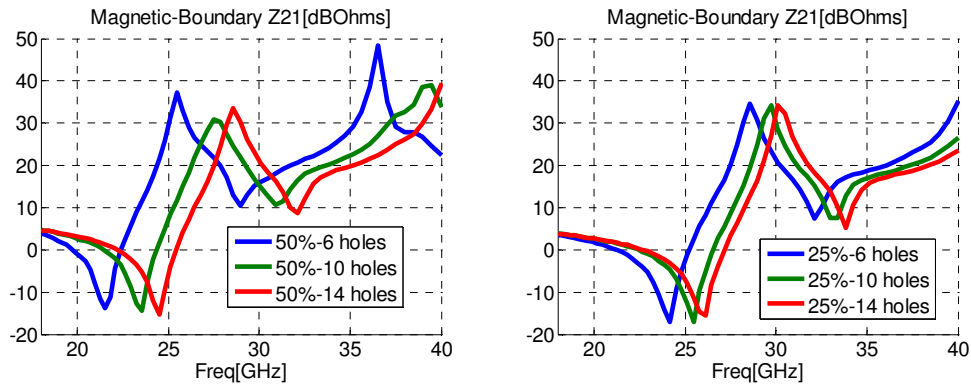


Figure 12: (Left) 50% perforation case, with 6, 10 and 14 holes per side.
(Right) 25% perforation case, with 6, 10 and 14 holes per side

As we cut holes on planes, the static plane pair capacitance decreases while the loop inductance increases. Based on the results shown in Figure 12, we can conclude that the increased loop inductance offsets the reduction of plane capacitance pushing the series resonance to a lower-frequency.

The first parallel resonance is also pushed to a lower frequency indicating the plane has an "apparent" bigger size as the waves have to travel around the holes to get to the boundary. Another interpretation is to consider these planes as periodically loaded planes. This loading is ultimately making the cavity propagation slower and hence reducing the first parallel resonance frequency.

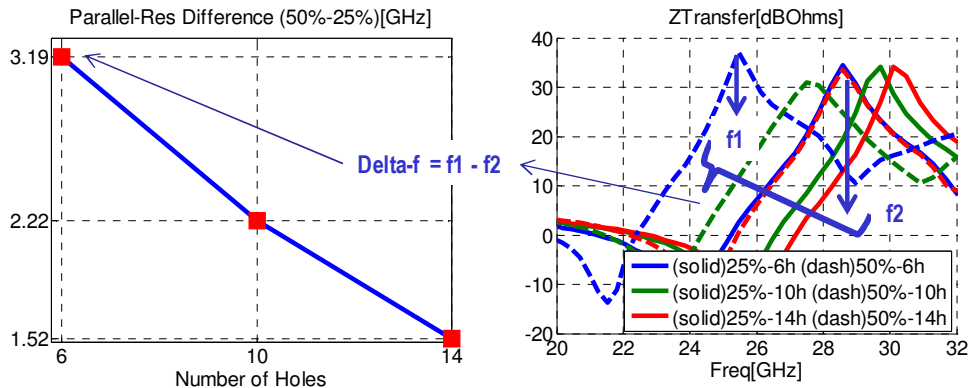


Figure 13: (Left) Parallel resonance frequency delta for different number of holes.
(Right) Transfer impedance for the 25%, 50% perforation, 6, 10, 14 holes.

Note that computing the parallel resonance delta between the 50% and 25% cut cases results in the 6 hole case having the largest frequency delta, followed by the 10 holes and finally the 14 hole case. This again points strongly to the fact that the size of the hole, not the number of them, is the predominant aspect that pushes the resonance to a lower frequency.

3.0 Test Structure

In previous sections we have explained, by means of simple examples, some of the important theory and considerations to be taken into account when analyzing via problems in multi-layer boards. In this section we'll present the test board used to take VNA measurements. Through measurements and simulations, we'll analyze the S-parameter results and relate them to the theory presented in section 2.

3.1 Test Board Description

Due to the increased number of voltage rails, high currents and routing density requirements of today's designs, it's not uncommon to find stack-ups with a dominant number of power-planes as is the case of our test board shown in Figure 14. The test board has two ground planes. All internal planes are used for power delivery. Even though, for many reasons this stack-up might not be ideal, it offers us a good, diverse, and rich corner case to study.

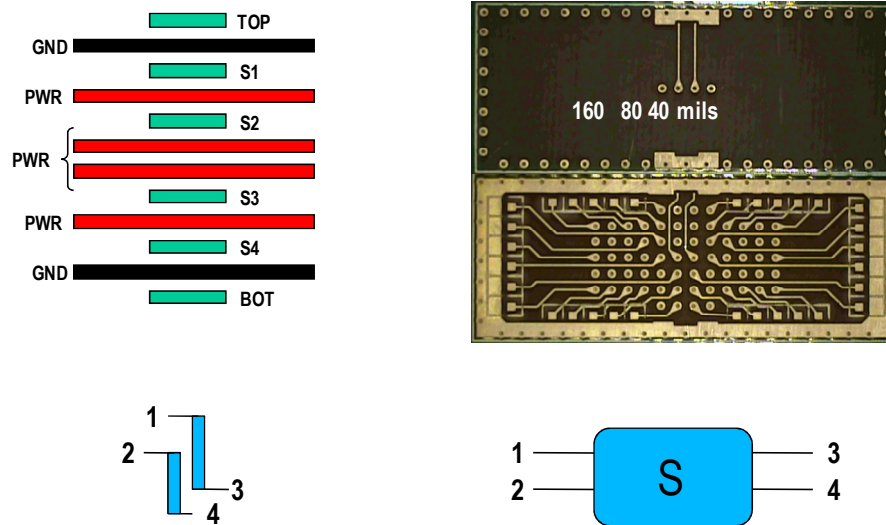


Figure 14: (Top left) Test board stack-up. (Top right) Test board photos, 2 grounds at 40mils separation, perforated and non perforated. (Bottom left) Port numbering for the two via case, (Bottom right) Port numbering, S-parameter circuit representation

The board size is 1020x400mils. The periphery was surrounded with ground vias tying the external ground planes together. Two signal vias are placed in the middle of the structure on a through measurement configuration. Two small micro strip lines are routed from the vias to the periphery of the board for measurement, as shown in Figure 14.

With the two signal vias and the surrounding periphery ground vias always present, different cases were created:

- Two signal vias without any ground vias nearby
- One ground via, separated by 40, 80, 160mils from the left signal via
- Two ground vias, one on each side, separated by 40, 80, 160mils from the signal vias (as shown on Figure 14)
- Two ground vias, on a perforated array, one on each side, separated by 40, 80 and 160mils. The added vias create perforations on the array and can be terminated with a single 50Ohm either on top or bottom (as shown on Figure 14)

In addition to the main cases, the test board was manually modified, for example by changing termination values on the perforated case; or by back-drilling some of the ground vias. These special cases will be detailed later in its own specific post-processing section.

Since a lot of S-parameters will be analyzed in the next sections, please refer to Figure 14 for the port number nomenclature

It's important to highlight that although the via pattern resembles a differential pair, we will in most cases treat it as single ended, looking at crosstalk between the vias. In uniform BGA array patterns, two legs of individual differential pairs can be facing each other similar to this test structure.

3.2 Data Post-Processing

Let's first analyze the difference between the no-ground, 1-ground and 2-ground cases with 40mil separation between signal and ground vias.

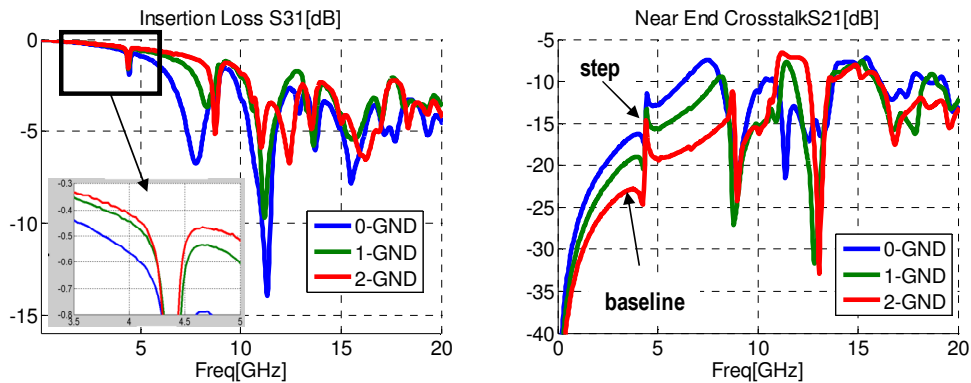


Figure 15: (Left) Insertion loss, for no-ground, one and two ground cases separated with 40mils. (Right) Near end crosstalk for the same cases.

Figure 15 shows the insertion loss and near end crosstalk measurements results of these three test cases. These results are rich in features. Let's analyze each feature, one at a time.

- Insertion loss and near-end crosstalk resonance dips:

The boundary resonances in this structure are one of the dominant aspects of the s-parameters results, as can be seen by the insertion and near end crosstalk dips in Figure 15. Two distinct types of boundaries can be identified in this structure:

- Open plane boundary between the internal power planes, and internal power to external ground planes (refer to Figure 14)
- Closed plane boundary between the two outer most ground planes shorted by the surrounding periphery vias.

To understand the effect of these two boundaries on the same structure, let's consider the case with two ground vias next to signal vias. With the help of the analytical via model shown in [1], [2] (with a slight modification), we can prove which one is the dominant cavity in this problem. The steps followed to generate such a via model are shown in Figure 16.

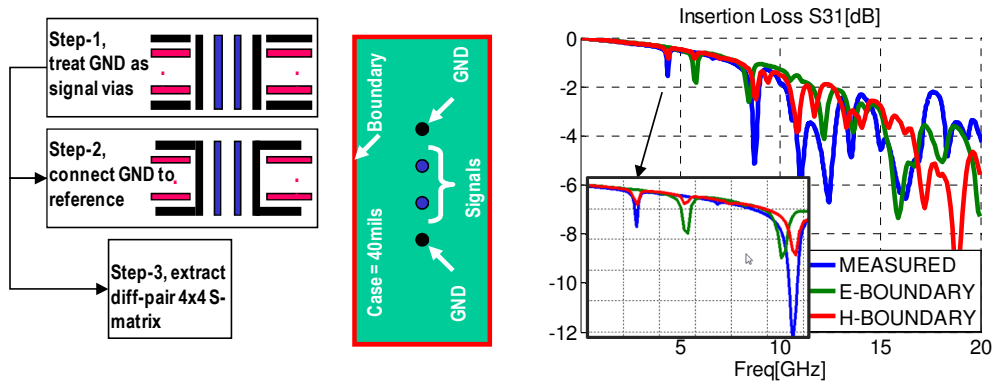


Figure 16: (Left) Analytical model steps and diagram. (Right) Comparison between measurement and the analytical model's electric, and magnetic boundary conditions

Step 1: Calculate the cavity analytical via model following [1], [2], but consider the nearby ground vias as signal vias. This will result in an 8x8 S-parameter matrix, with a total of four vias.

Step 2: We know that the ground vias only connect to the top and bottom ground planes. This can be achieved by renormalizing the S-parameter matrix with different terminal impedance values for the signal vias vs. the ground vias. A renormalization impedance of 50 ohms was used for the signal vias, and a renormalization of 0.01Ohm was used for the

ground vias. By doing this, we are in essence connecting the two ground vias together at the ground plane locations to the absolute analytical reference.

Step 3: Since we are only interested in the signal via S-parameters, the $S_{4 \times 4}$ sub-matrix was extracted from the $S_{8 \times 8}$ complete matrix and used to overlay against the measurement data.

By performing the modification to the analytical formulation, via models with ground connected only on some planes can be created. Then, by changing the boundary condition of the analytical model from magnetic (H) to electric (E), we can observe the different resonance locations. Figure 16 shows, when we consider a magnetic boundary (H), the analytical resonance results properly align with measurements. On the other hand, electric boundary (E) analytical resonance results do not.

As expected, the external ground plane cavity formed with shorted ground vias is broken by all the other internal planes; hence the resonances on the "surrounding-PEC" cavity can't be developed, only the open (magnetic) boundary is present.

- Insertion loss difference at low frequency (up to 5GHz):

Figure 15 also shows the insertion loss up to 5GHz (before the first plane resonance). The 0-ground case insertion loss is bigger than the 1-ground case, which in turn is bigger than the 2-ground case. This is explained by understanding that the ground vias act as a shield and a return current path, even though they connect to only two planes. The nearby ground vias contain the signal energy keeping it from diverging to the boundary periphery. In the 0-ground case, all the energy is sent to the boundary, and hence the impedance of the return current path is higher than the other cases, so we observe the increase of insertion loss starting earlier.

- Near End Crosstalk baseline and jump:

Analyzing the near-end crosstalk curves in Figure 15, we notice two important signatures; a baseline, and a step. In the 0-ground via configuration, a lot of the energy is coupled to the other via and we can see a higher baseline. In contrast when we have two grounds the amount of energy coupled to the adjacent via is less and this results on a smaller baseline. The steps are similar in size and are produced by the energy being reflected from the boundaries. The step frequency is the same as the insertion loss resonance dip, as expected.

Changing gears, another aspect to understand is the effect of ground to signal vias separation. Figure 17 shows the two ground via case comparison, including all ground to signal via separations. These cases have also been compared to the no-ground case as a baseline for reference.

We start by noticing the insertion loss of the 160 mil ground separation case starts to approximate closely the 0-ground case. The near end crosstalk difference between these two cases is very small. In short we conclude that on a typical stack of approximately 90mils of thickness, where the separation between ground to signal is greater than 3 times the separation between signal vias, the ground via has a negligible effect on crosstalk and via insertion loss. On the other hand, when the ground to signal via separation is less than 2 times the signal to signal via separation, a noticeable effect can be observed; the baseline, and overall crosstalk is reduced and insertion loss improved.

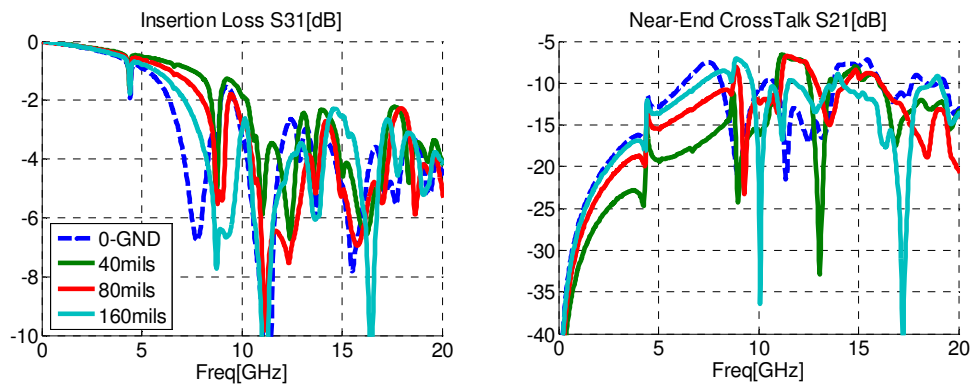


Figure 17: (Left) Insertion loss on the 2 ground cases, for all distances, 40mils, 80mils and 160mils, including the 0 ground case as a reference. (Right) Same as left, for near-end crosstalk

Many times we are confronted with the decision of replacing ground vias for power vias. To mimic this effect on our test board, one of the ground vias of the 2 ground case was backdrilled just enough to disconnect one of the ground plane connections as shown on Figure 18.

Looking at the insertion loss results, we note the resonance dip on the back-drilled case (BD) is more pronounced than the 1 ground and 2 ground cases. The simulated “power via” (back-drilled ground via) is to some extent amplifying the insertion loss resonance dip. It’s important to realize the back-drilled ground via, or any power via connection to one plane on one side, has low impedance on the plane connection side, and high impedance on the open side. These types of structures are quarter wave resonators as will be shown later.

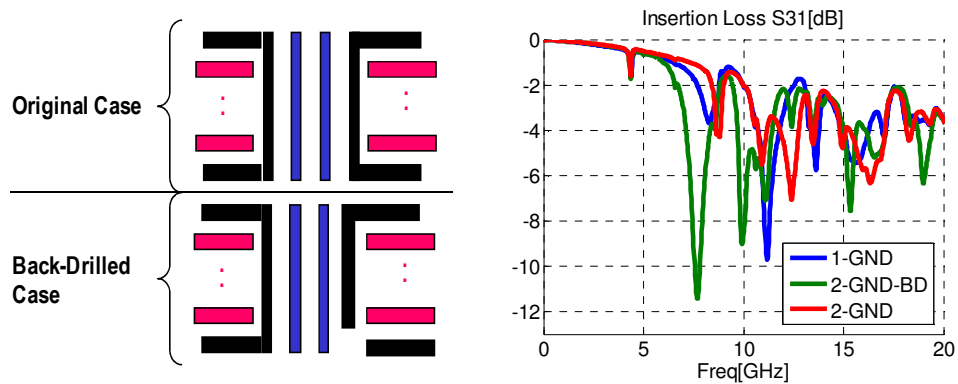


Figure 18: (Left) Example of backdrilled ground via case. (Right) Insertion loss of the 40 mil 2-ground case, normal and backdrilled, and the 1-gnd case as a reference.

Finally, the fully perforated 2 ground via case, with 40 mil ground separation was measured as shown in Figure 19. In this structure there are 60 additional signal vias, terminated on either the top or bottom layer to 50 ohms as shown in Figure 14. In this case, the insertion loss profile is flatter with less dips even though the boundary hasn’t been changed. Also, the near end crosstalk step previously observed on the full un-perforated plane is not present anymore.

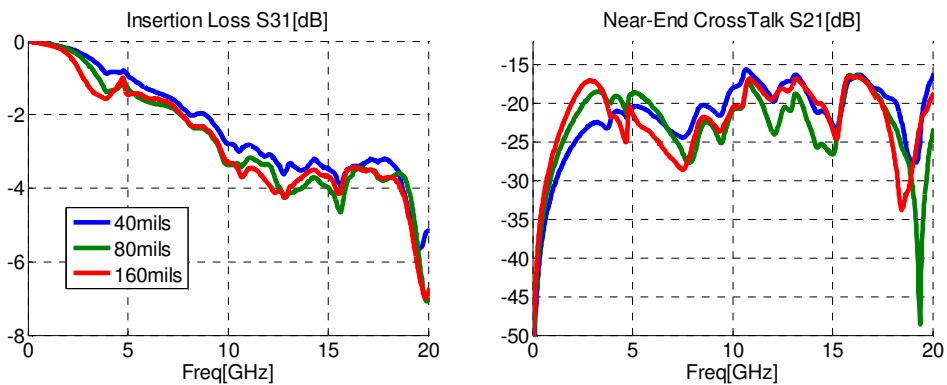


Figure 19: (Left) Insertion loss for all ground separations of the perforated 2-ground case (Right) Same as left, for near-end crosstalk

To further highlight the differences between the perforated versus non perforated plane case, the S-parameters results of the two ground vias at 40 mil separation was overlaid as shown in Figure 20. There are two important differences to highlight between these cases:

1. The perforated plane does not show all the insertion loss and near end crosstalk resonance dips as compared to the non perforated case
2. The perforated plane shows more attenuation on the insertion loss than the non perforated case

The perforated case, with all signals vias terminated with 50 ohms, is disrupting and absorbing the plane resonances. Reflections from the boundaries do not return to the signal vias as strongly and hence the resonance dips disappear. Also

since the energy is absorbed, the perforated case has more overall attenuation. The same behavior is observed in the near end crosstalk. The step is not present because the boundary resonance is disrupted.

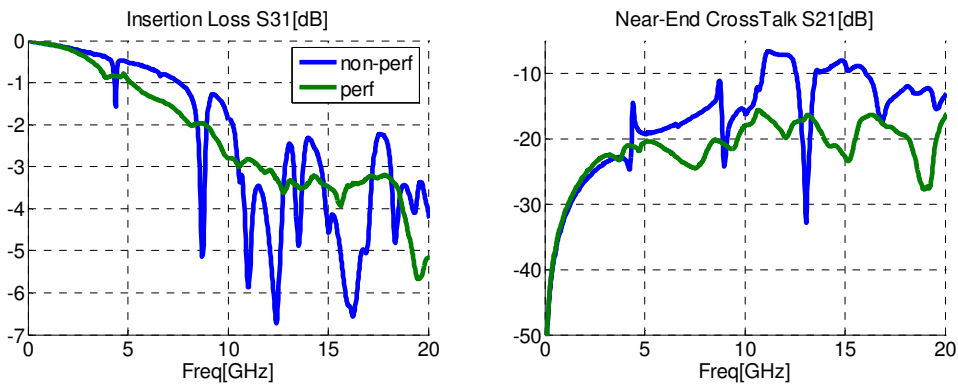


Figure 20: (Left) Insertion loss comparison between the perforated and non-perforated 40mil 2 ground separation case. (Right) Same as left for near-end crosstalk

The remaining question on the perforated case is whether the absorption of energy is simply due to the presence of the vias, or rather, the fact that the vias were terminated to 50 Ohms and the termination is absorbing the energy. In order to prove this point, a measurement on the perforated plane was taken in two additional steps; first increasing all the extra signal vias terminations from 50Ohms to 100Ohms and then removing the terminations on the extra vias completely.

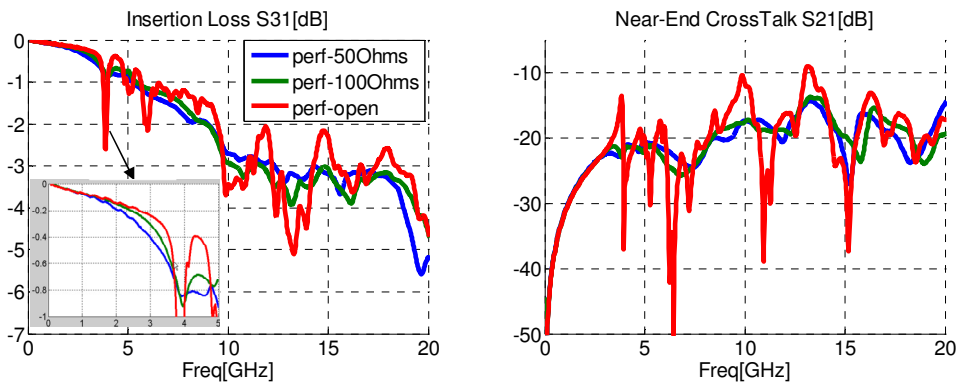


Figure 21: (Left) Insertion loss comparison between perforated cases, with 50ohms, 100Ohms and no termination. (Right) Same as left for near end crosstalk

Figure 21 shows the difference between these perforated cases. Note the similarity in the 50 Ohm and 100 Ohm termination cases. Conversely, the open case again contains large resonance dips and less attenuation. The resonances in this figure are not produced by the plane boundaries, but rather from the vias and traces attached to the unpopulated termination resistors. In the case of 50 Ohms these traces are terminated and no resonances occur. For 100Ohms we begin to observe a small resonance dip. It is also observed that the unterminated case has less overall attenuation than the others, supporting the theory that the main absorption element on the pin field, comes from the via terminations and not necessarily from the presence of the vias.

In conclusion, terminated pin fields will break and absorb plane resonances, but at the same time they will increase the insertion loss attenuation on signal vias. This also implies the response of a signal via placed on a pin field edge, in a boundary proximity, will be very different than the response of another via in the middle of the same pin field.

3.3 Measurement Correlations

In the previous section, we've analyzed measured cases and introduced a simple modification of the cavity analytical model as a cross-check exercise. In this section, a few of the most complex measured structures will be simulated in a 3D field solver to establish correlation. Good correlation on the most complex cases will serve to increase our confidence level on the modeling techniques and will be the stepping stone to build other more realistic differential cases.

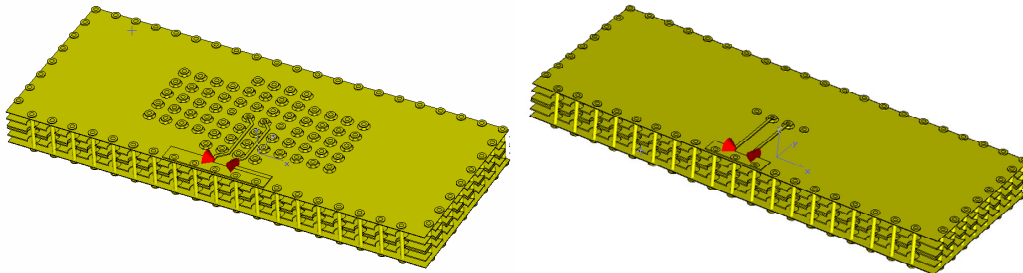


Figure 22: (Left) Physical model of the perforated, 2 ground 40 mil separation case. (Right) Same as left for non-perforated case.

Two cases were modeled for measurement correlations. Figure 22 shows the perforated and non-perforated case, both with two grounds separated 40 mils from the signal vias.

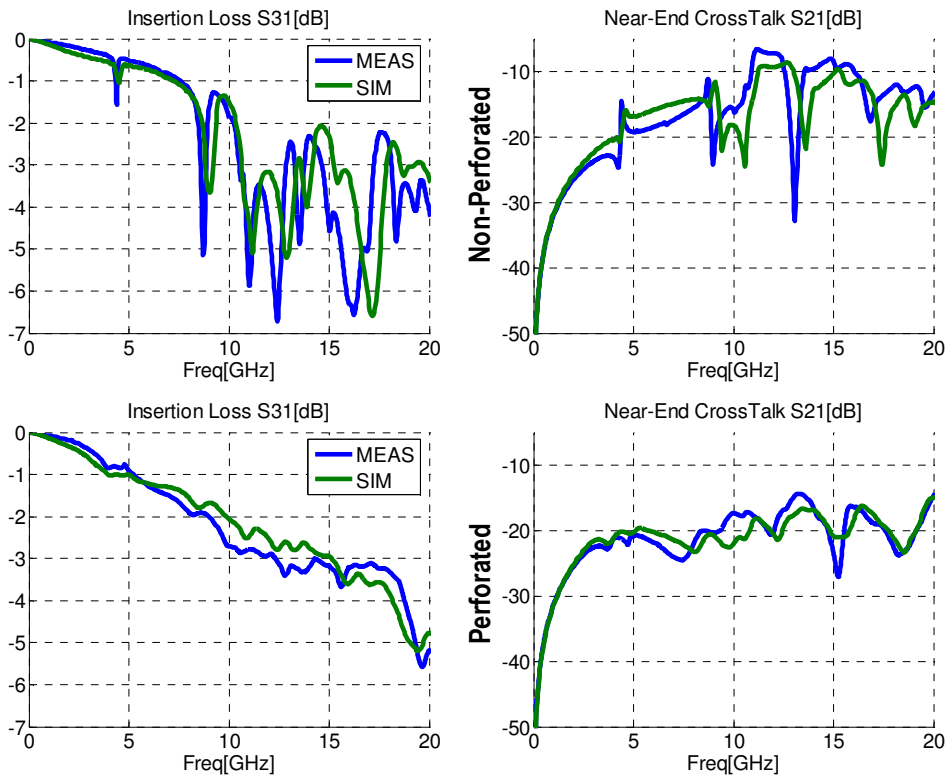


Figure 23: (Top-Left) Non-perforated insertion loss correlation. (Top-Right) Non-perforated near-end crosstalk correlation. (Bottom-Left) Perforated insertion loss correlation. (Bottom-Right) Perforated near end crosstalk correlation

As can be seen in Figure 23, the simulation results are very accurate and able to capture not only the trends but also the absolute values in good detail. After achieving this level of correlation, we can now explore other cases and see how crosstalk and cavity coupling will behave in various differential pair scenarios.

4.0 Differential Via Crosstalk In The Presence of Power Vias Stubs

The objective of this section is to show how differential crosstalk between vias may be affected by the presence of nearby ground and power vias. To achieve this goal, two baseline structures (Figure 24), including three differential pairs each, will be analyzed. One of the cases has the differential pairs offset from each other. The other case has the vias facing each other without offset. The pitch between vias is 39.37mils (1mm). This analysis has been done using a stack-up rich in power and ground planes with 22 layers and approximately 93mil overall thickness.

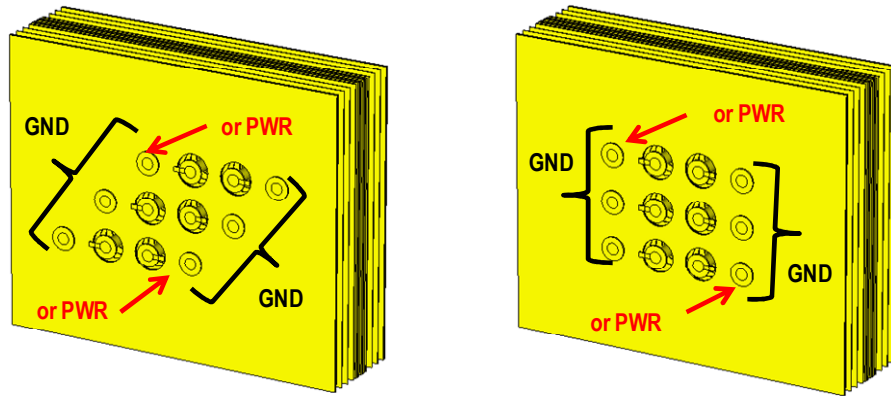


Figure 24: (Left) Offset via pattern showing ground vias replaced by power-vias for different simulation cases, (B1, B1_PT, B1_PM, B1_PTB). (Right) Same as left for straight via pattern (B2, B2_PT, B2_PM, B2_PTB).

In order to capture the effect power vias have on crosstalk, different simulations were run including power vias connected to different plane layers. Only three of the more relevant power-planes of this study are shown together with the stack in Figure 25. All of the simulation cases, including the baselines, are listed in table 1 below.

Case Name	Description
B1	Offset via pattern surrounded by 6 ground vias as shown in Figure 24 (left). (Baseline case)
B1_PT	Offset via pattern, replacing two ground vias with power vias connected to the top power plane, (PT)
B1_PM	Offset via pattern, replacing two ground vias with power vias connected to the middle power plane, (PM)
B1_PTB	Offset via pattern, replacing two ground vias with power vias connected to the top and bottom power planes (PT,PB)
B2	Straight via pattern surrounded by ground vias as shown on Figure 24 (right). (Baseline Case)
B2_PT	Straight via pattern, replacing two ground vias with power vias connected to the top power plane, (PT)
B2_PM	Straight via pattern, replacing two ground vias with power vias connected to the middle power plane, (PM)
B2_PTB	Straight via pattern, replacing two ground vias with power vias connected to the top and bottom power planes, (PT, PB)

Table 1: Description of differential via crosstalk simulation cases

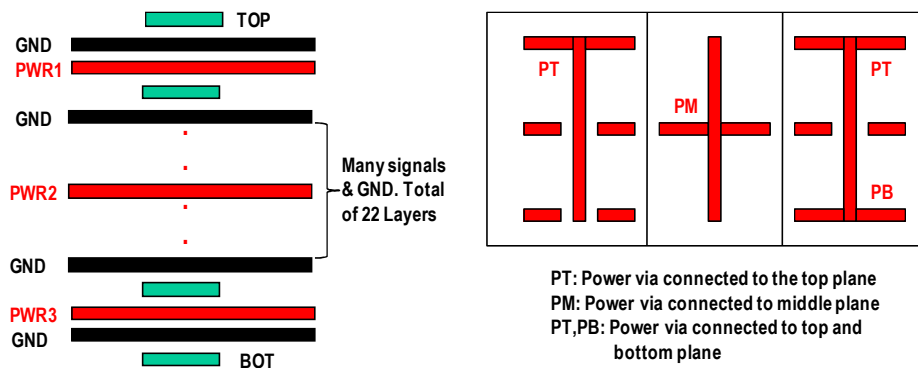


Figure 25: (Left) Stack-up used for the differential via crosstalk simulations. (Right) Power-via connection cases, three different power via connection schemes shown.

First, let's review the results from a "single-ended" view point. In Figure 26, the insertion loss of B1, B1_PT, B1_PM and B1_PT B are compared. The baseline case B1 shows the smallest unperturbed insertion loss and near end crosstalk profile. In contrast the B1_PT case shows an steep resonance around 10GHz. The same effect is encountered with the near end crosstalk profile. At 10GHz the single ended coupling between the adjacent vias of separate differential pairs reaches a maximum

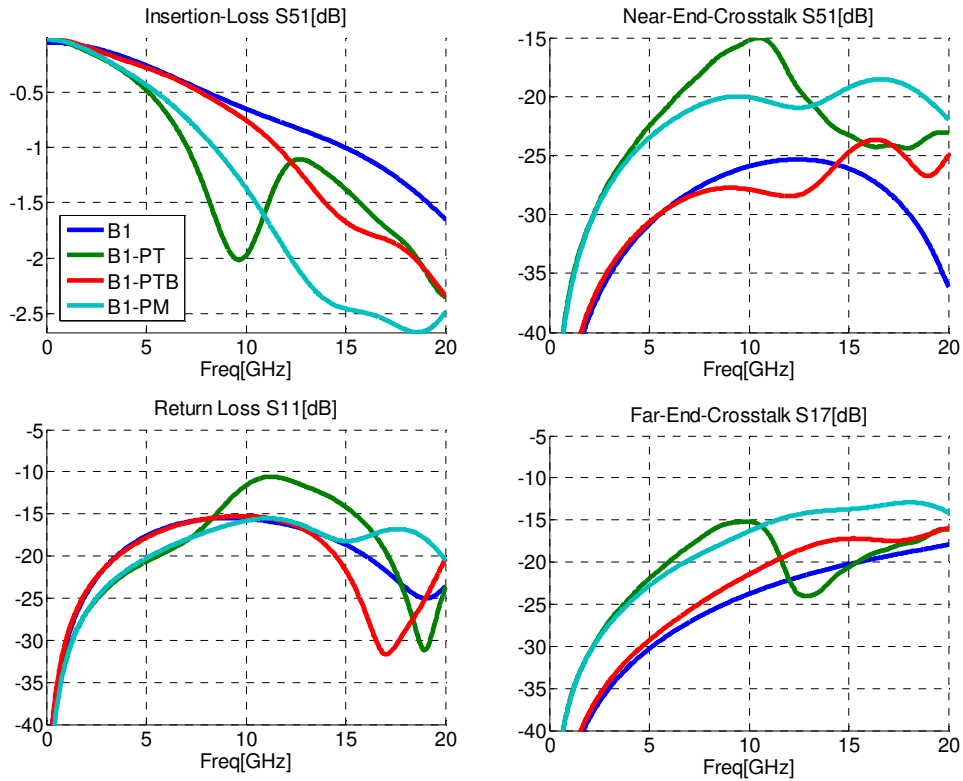


Figure 26: Offset case, different power via connection comparison (Legend in the top-left figure indicate the case).
 (Top Left) Single ended insertion loss. (Top Right) Single ended near end crosstalk.
 (Bottom Left) Single ended return loss.(Bottom Right) Single ended far end crosstalk

Looking at the bottom plane E-field for the B1_PT case (Figure 27) we notice that the signal via injecting the current into the cavity couples strongly to the power via nearby. Further data post-processing shows the insertion loss dip and the near end crosstalk peak frequency occurs at a 1/4 wavelength of the power via. This effect is the same as the notorious stub effect of signal vias, now observed through cavity coupling to power vias.

Notice that when the power via is connected on one side to a low impedance power plane, and on the other side it's left open, the structure sustains a quarter wave resonance. The B1_PT case shows a much better performance since the power via is now connected at both ends, allowing only a half wavelength resonance frequency. In this case a smaller dip at higher frequencies can be observed. The B1_PM case, since it's connected to only one plane, supports a 1/4 wave resonance. The resonance frequency in this case is also pushed higher, since the length of the stub is approximately half, as compared to the B1_PT case.

Though common mode effects for differential pairs are important and need to be considered, the fundamental concern is the differential propagation on each pair. By replacing two ground vias with power vias in this configuration, asymmetries are introduced into the structures forcing a degradation of differential transmission.

We can directly see this effect on the S-parameters by converting the eight port single ended matrix into a coupled eight port mixed mode matrix and examining the mixed mode differential quadrant.

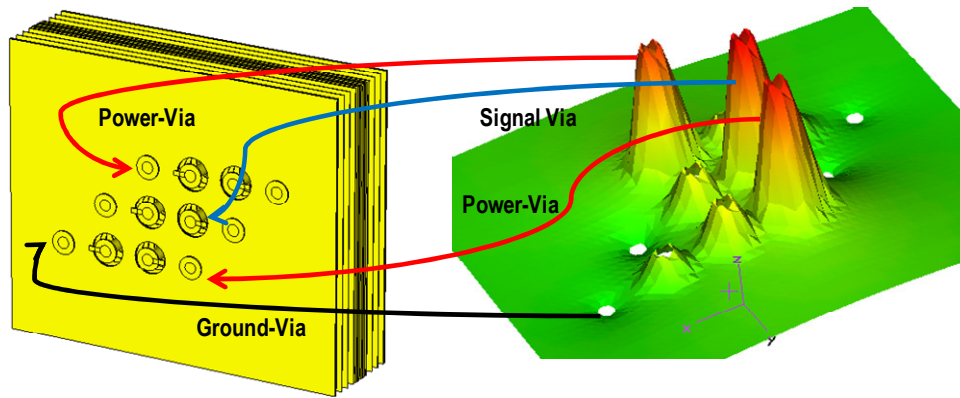


Figure 27: (Left), physical model of the offset case. (Right), planner E-field at top plane

The mixed-mode differential insertion loss in Figure 28 clearly shows a resonance at 10GHz, both in the insertion loss and near end crosstalk. Between the B1 and B1_PT cases, a 10dB difference can be observed at 10GHz on the near end crosstalk. It's also interesting to see the B1_PM case showing the resonance frequency at around twice the frequency of the B1_PT case. This is expected since there are two quarter wave resonators in parallel with half the length, hence double the frequency.

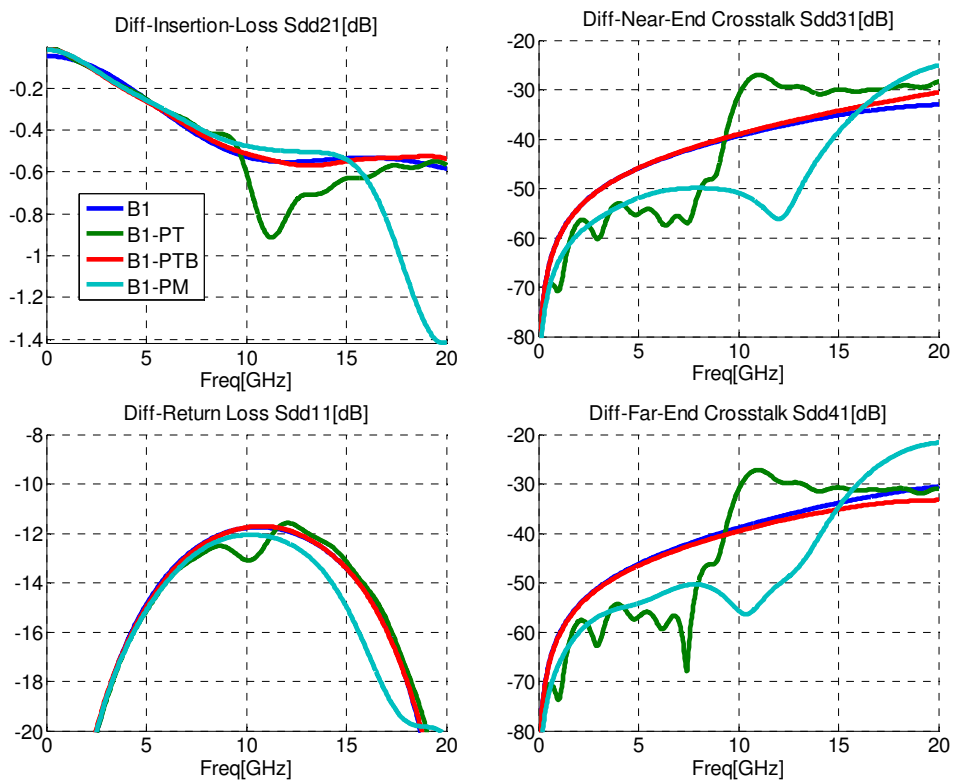


Figure 28: Offset case, different power via connection comparison (legend on the top-left figure indicates case).
 (Top Left) Differential insertion loss. (Top Right) Differential near end crosstalk.
 (Bottom Left) Differential return loss. (Bottom Right) Differential far end crosstalk

So far, all the previous examples examined are B1 cases. In Figures 29 and 30 we compare the B1 to B2 cases for all the different power connections.

In Figure 29 it can be observed that the B2_PT case differential insertion loss dip is smaller than the B1_PT case. This is to be expected since the relative location of the power via with respect to the differential pair produces less asymmetry. Also the near end crosstalk shows the excursion of the B2_PT case is less but the overall crosstalk is higher. This is also to be expected since all the differential pairs face each other in close proximity.

When we compare the B1 and B2 baseline cases, we see similar trends; the insertion loss is very similar for both cases, but the near end crosstalk is higher on the B2 case.

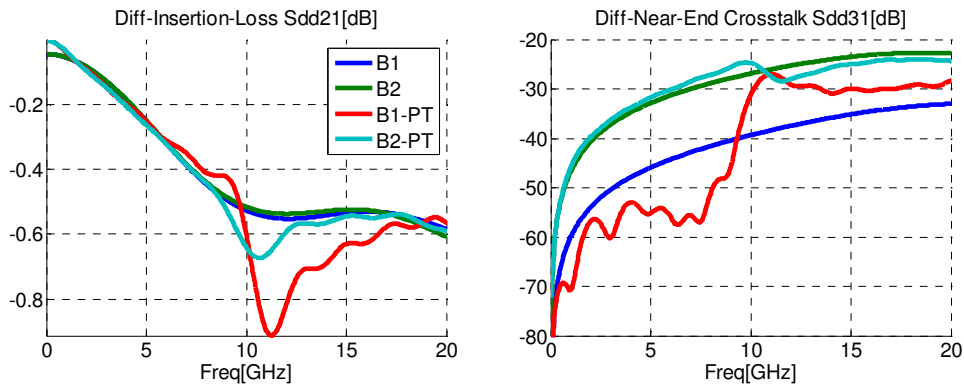


Figure 29: Comparison between offset (B1) and straight (B2) cases (legend on the-left figure indicates case). (Left) Differential inserion loss. (Right) Differential near end crosstalk.

In Figure 30, the remaining cases have been compared. If we analyze the B1_PM and B2_PM cases, we see the dip is very pronounced on the B1_PM case, but not as pronounced on the B2_PM case. As previously explained, the B1_PM physical structure is more asymmetrical than the B2_PM structure. The important point to note here is that although the dip is smaller, it's still present on the B2_PM.

In terms of near-end crosstalk, we see the same effect, where the B2_PM case has an overall higher coupling due to the closer via proximity.

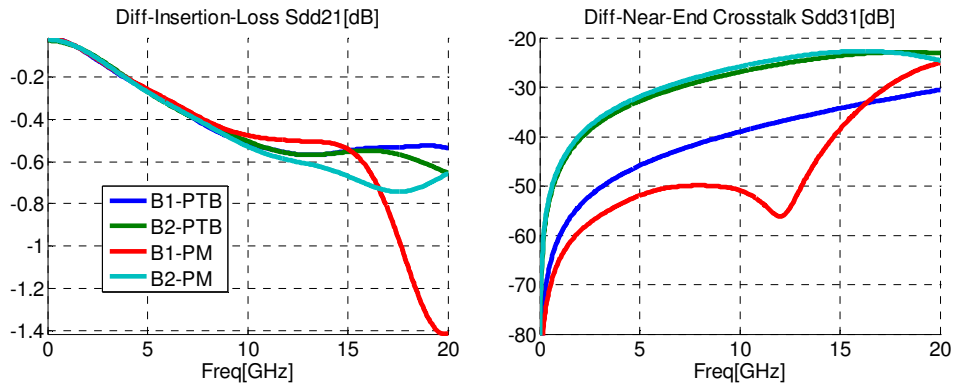


Figure 30: Comparison between offset (B1) and straight (B2) cases (legend on the-left figure indicates case). (Left), differential inserion loss. (Right), differential near end crosstalk.

In this section we've shown that power vias will also resonate depending how they are connected into the stack. When considering the use of a power via as a differential pair reference, it's important to note that depending on which plane layer the power via is connected, the via can experience either a quarter wavelength or half wavelength resonant frequency that will exacerbate crosstalk between signal vias.

5.0 Conclusions

In this work, we have stressed the fact that cavities are one of the most important structural aspects that contribute to signal via coupling. By understanding the cavity coupling mechanism, we can understand the interaction between vias.

The following list is a summary of all the aspects and conclusions that have been covered in this work:

- With the help of theoretical examples we've shown how signal via coupling occurs in cavities and with a simple equation we demonstrated how to compute the crosstalk directly on the structure from the E-field.
- Proper boundary selection is key to obtain accurate models in 3D via simulations. It's common for 3D models to be characterized using absorbing boundary (no reflections from the edges). In many cases, this may be a good approximation, for example when the via analyzed is in the middle of a large board or the middle of a pin field array. In other cases it may not, for example, when signal vias are placed on small planes, or close to edges.
- It has been shown that on heavily perforated planes, the cavity resonances shift to lower frequencies as compared to the full plane. This is due to the periodically loaded characteristics of the perforated plane. It has also been observed from simulations that perforation size has a greater impact than the number of perforations for the same amount of area removed.
- A simple modification to the analytical cavity via model has been proposed, to show how to account for either ground or power vias connecting to an arbitrary number of planes.
- Through measurements, we've seen the behavior of insertion loss and crosstalk between signal vias change dramatically depending on whether the via is in isolation or in the middle of a pin field array. In via fields, such as a BGA, most of the resonances are dampened and the signal via insertion loss is increased.
- We've analyzed the impact of ground to signal via separation with respect to crosstalk and insertion loss (return current path). It's been shown that when the ground to signal via separation is more than 3X the signal to signal via separation, little ground via effect can be observed both in the insertion loss and crosstalk profiles. More appreciable differences can be observed when the ratio is less than 2X. We've outline the mechanism by which the nearby ground vias serve as a return current path and allows the signal via to improve its insertion loss response.
- We've shown by way of measurement and simulation that stubs on power vias can also resonate, helping propagate crosstalk between signal vias. When deciding to replace ground with power vias, it's important to understand that the location of the via is not the only important consideration; the layer, or layers where the connection occurs is of paramount importance.
- We've shown that a power via connecting to only one plane acts as a quarter wave resonator similar to the well known "signal stub via". If the plane connection is on the top or bottom of the stub, the quarter wave resonator length will be such that the resonance will be present at lower frequencies. When connecting the via to multiple layers, different resonance patterns can be formed, but resonances will occur at higher frequencies.

Acknowledgement

The authors wish to extend their thanks to Eugene Whitcomb (SUN) for his help in creating and preparing the sample structures.

References

- [1] Christian Schuster, "Developing a Physical Model for Vias", Proc. of DesignCon 2006, Jan.31-Feb.3 2006, Santa Clara, CA.
- [2] Giuseppe Selli, "Developing a Physical Model for Vias - Part II: Coupled and Ground Return Vias", Proc. of DesignCon 2007, Jan.29-Feb.1 2007, Santa Clara, CA.
- [3] Istvan Novak, "Measurement of Power-Distribution Networks and Their Elements", Proc. of DesignCon East 2003, Jun.23-Jun.25, Marlborough, MA
- [4] Novak, Miller, "Frequency Domain Characterization of Power Distribution Networks", 2007 Artech House, INC. ISBN-13:978-1-59693-200-5
- [5] Jason R. Miller, Istvan Novak, "Characterizing and Modeling the Impact of Power/Ground Via Arrays on Power Plane Impedance", Proc. of DesignCon 2005, Jan.31, Feb 3, Santa Clara, CA.